PHOTOCATALYTIC PERFORMANCE OF ZnO NANOROD COUPLED PHOTOCATALYSTS UNDER FLUORESCENT LIGHT AND SUNLIGHT IRRADIATION FOR PHENOL AND 2,4-DICHLOROPHENOXYACETIC ACID DEGRADATION

by

LAM SZE MUN

Thesis submitted in fulfillment of the requirements
for the degree of
Doctor of Philosophy

AUGUST 2014

ACKNOWLEDGEMENTS

I would like to convey my deepest appreciation to my main supervisor, Prof. Dr. Abdul Rahman Mohamed for his constant encouragement, invaluable guidance, patience and understanding throughout the whole length of my PhD candidature. This project had been a tough but enriching experience for me in research. I would like to express my heartfelt thanks to my co-supervisor, Assoc. Prof. Dr. Ahmad Zuhairi Abdullah for his guidance on my research work.

I would like to express my sincerest appreciation to the management, especially Dean, Prof. Dr. Azlina Bt. Harun @ Kamaruddin, Deputy Dean, Assoc. Prof. Ahmad Zuhairi Abdullah and all the staff members of School of Chemical Engineering for granting me a good environment to perform my research work. Thanks also go to the staffs of School of Material and Mineral Resources Engineering, School of Biological Science and School of Chemical Science for their assistance on sample analyses. I am also grateful to Prof. Dr. Tadashi Itoh and Assoc. Prof. Dr. Satoshi Ichikawa for their support during my stay in Japan for the HRTEM analysis in this PhD project. At the same time, I am greatly appreciated the USM Research University (RU) grant (no. 814174), USM Postgraduate Research Grant Scheme (PRGS) (no. 8045030) and Malaysia MyPhD scholarship for providing me the financial support during the course of the study.

Most importantly, I would like to thank my father Lam Fook Cheon and my mother Kan Lai Leng for their continuous support during my PhD study. Special thanks also given to all of my lab mates and friends: Sin Jin Chung, Rohaiya, Yeoh Wei Ming, Seah Choon Ming and Lee Kim Yang, who have helped me in different ways in my work and make my stay in USM more enjoyable.

TABLE OF CONTENTS

LIST OF TABLES

LIST OF FIGURES

LIST OF PLATES

LIST OF SYMBOLS

Symbol	Description	Unit
C_t	Concentration at time *t*	mg/L
C_o	Initial concentration	mg/L
c	Velocity of light	m/s
CB	Conduction band	-
D	Crystallite size	nm
d	Lattice spacing	nm
e^-	Electron	-
E_g	Band gap energy	eV
E_{phot}	Photon energy	eV
h^+	Hole	-
h	Planck's constant	eVs
H	Hysteresis	-
HO_2•	Hyperoxyl radical	-
hv	Photon energy	-
K_a	Adsorption equilibrium constant	L/mg
k_{app}	Apparent rate constant	1/min
k_r	Reaction rate constant	mg/L.min
O_2•$^-$	Superoxide radical anion	-
OH^-	Hydroxyl ion	-
•OH	Hydroxyl radical	-
P	Pressure	Pa
P_o	Initial Pressure	Pa
r_o	Initial reaction rate	mg/L.min
r	Reaction rate	mg/L.min
R^2	Correlation coefficient	-
VB	Valence band	-
zpc	Zero point of charge	-
λ	Wavelength	nm
θ	Bragg's angle in degree	-
β	Full-width at half maximum (FWHM)	-

LIST OF ABBREVIATIONS

AAS	Atomic absorption spectrophotometer
AOPs	Advance oxidation processes
BET	Brunauer-Emmett-Teller
$BaSO_4$	Barium Sulphate
CO_2	Carbon dioxide
CuO	Copper (II) oxide
1D	One dimensional
DI	Deionized water
EDCs	Endocrine disrupting chemicals
EDX	Energy dispersive X-ray
EHP	Electron and hole pair
E_{EO}	Electrical energy per order
H_2SO_4	Sulphuric acid
HNO_3	Nitric acid
H_2O	Water
H_2O_2	Hydrogen peroxide
HPLC	High performance liquid chromatograph
HRTEM	High resolution transmission electron microscopy
IPA	Isopropanol
IC	Ion chromatography
L–H	Langmuir-Hinshelwood
O_2	Oxygen
p-BQ	*p*-Benzoquinone
PL	Photoluminescence
PTFE	Polytetrafluoroethylene
MO_x	Metal oxide
N_2	Nitrogen
Nb_2O_5	Niobium pentoxide
NaI	Sodium Iodide
NaOH	Sodium hydroxide
NHE	Normal hydrogen electrode

TA	Terephthalic acid
TiO_2	Titanium dioxide
TEM	Transmission electron microscopy
TOC	Total organic carbon
USEPA	United State Environment Protection Agency
UV	Ultraviolet
UV–vis DRS	Ultraviolet-visible diffuse reflectance spectrophotometer
WO_3	Tungsten trioxide
XRD	X-ray diffraction
Xe	Xenon
2,4-D	2,4-Dichlorophenoxyacetic acid
ZnO	Zinc oxide

PRESTASI PEMFOTOMANGKINAN BAGI FOTOPEMANGKIN BERPASANGAN ZnO ROD NANO DI BAWAH PENYINARAN LAMPU PENDAFLOUR DAN CAHAYA MATAHARI UNTUK DEGRADASI FENOL DAN ASID 2,4-DIKLOROFENOKSIASETIK

ABSTRAK

Selama bertahun-tahun, aktiviti perindustrian yang pesat masih menjadi satu cabaran yang rumit bagi kebanyakan negara. Aktiviti perindustrian yang tidak dapat dielakkan ini menyebabkan peningkatan bahan pencemar ke dalam alam sekitar. Fotopemangkinan heterogen, terutamanya pada logam oksida digandingkan dengan satu dimensi (1D) ZnO berbentuk rod nano (MO_x/ZnO) bertindak sebagai fotopemangkin heterostruktur yang berkesan telah digunakan untuk merawat dua bahan pencemar kimia pengganggu endokrin (EDC) iaitu fenol dan asid 2,4-diklorofenoxiasetik (2,4-D). Satu siri fotopemangkin MO_x/ZnO (MO_x = CuO, WO_3 and Nb_2O_5) dengan kedudukan jalur tenaga relatif yang berbeza di antara ZnO and MO_x telah dibangunkan. Fotopemangkin ini telah disediakan dengan kaedah hidroterma–pemendapan dan digunakan untuk fotodegradasi bahan pencemar yang dinyatakan di atas. Fotopemangkin WO_3/ZnO menunjukkan prestasi yang terbaik di antara tiga fotopemangkin yang dikaji dalam degradasi fenol di bawah penyinaran cahaya pendarfluor. Ia juga menunjukkan fotoaktiviti jauh lebih tinggi daripada ZnO tulen, ZnO komersial dan TiO_2 komersial di bawah keadaan yang sama. Selain itu, fotopemangkin yang dihasilkan ini juga menunjukkan potensi untuk kitar semula kerana ia boleh memendap di dalam larutan dalam masa dua jam selepas penyinaran dan aktiviti degradasi mereka masih lebih daripada 80% selepas empat kitaran. Fotopemangkin ini juga dianalisis oleh pelbagai teknik pencirian untuk mendapatkan ciri-ciri fiziko-kimia mereka. Pasangan oksida logam ini menurunkan jurang jalur

ZnO rod nano dari 3.24 eV ke 3.07–3.22 eV dan ini telah menyebabkan fotodegradasi beralih ke kawasan tampak. Fotopemangkin ini mempunyai luas permukaan yang besar untuk fotodegradasi dan ia juga merupakan isoterma jerapan-penyahjerapan nitrogen jenis IV dengan kelok H3 histerisis. Berbanding dengan ZnO tulen, spektra fotoluminasi (PL) bagi fotopemangkin MO_x/ZnO menunjukkan penurunan intensiti yang dramatik. Bagi fotopemangkin WO_3/ZnO, intensiti PL didapati paling rendah. Peningkatan fotoaktiviti bagi WO_3/ZnO adalah disebabkan oleh pemisahan pasangan e^- dan h^+ yang tinggi dan keupayaan potensi redoks yang dimiliki oleh dua semikonduktor untuk menghasilkan radikal •OH yang aktif. Ini telah dibuktikan dengan eksperimen pemungut radikal dan asid *terephthalic*–PL (TA–PL). Pelbagai parameter operasi seperti kepekatan awal pencemar, pH larutan, suhu pengkalsinan dan bebanan oksida logam berpasangan telah dikaji. Tahap degradasi dan penguraian EDCs juga disahkan oleh analisa HPLC dan TOC. Ujikaji kinetik mendapati tertib tindak balas yang menggambarkan penguraian EDCs di bawah cahaya pendarfluor adalah kinetik tertib-pertama berdasarkan model *Langmuir-Hinshelwood*. Penggunaan tenaga elektrik bagi setiap tertib magnitud untuk fotodegradasi EDCs adalah lebih rendah dengan menggunakan fotopemangkin WO_3/ZnO berbanding dengan TiO_2 komersial. Tambahan pula, fotopemangkin WO_3/ZnO juga boleh menggunakan cahaya matahari dengan berkesan untuk degradasi EDCs dan aktiviti fotopemangkinan mereka sekali lagi lebih baik daripada ZnO tulen dan TiO_2 komersial di bawah keadaan yang sama.

PHOTOCATALYTIC PERFORMANCE OF ZnO NANOROD COUPLED PHOTOCATALYSTS UNDER FLUORESCENT LIGHT AND SUNLIGHT IRRADIATION FOR PHENOL AND 2,4-DICHLOROPHENOXYACETIC ACID DEGRADATION

ABSTRACT

Over the years, the surge of industrial activities that inevitably resulted in an increasing flux of pollutants in the environment still remains an intricate challenge for nations. Heterogeneous photocatalysis, particularly on metal oxide coupled on one dimensional (1D) ZnO nanorods (MO_x/ZnO) as promising heterostructured photocatalysts were employed to treat two endocrine disrupting chemical (EDC) pollutants, namely phenol and 2,4-dichlorophenoxyacetic acid (2,4-D). A series of MO_x/ZnO (MO_x = CuO, WO_3 and Nb_2O_5) photocatalysts with different relative energy band positions between ZnO and MO_x were developed. The photocatalysts were prepared by a hydrothermal–deposition method and adopted in the photocatalytic degradation of the above mentioned pollutants. The WO_3/ZnO photocatalysts exhibited the best performance in the fluorescent light degradation of phenol among the three photocatalysts. It was also found that the photoactivities of developed photocatalysts were much higher than those of pure ZnO, commercial ZnO and commercial TiO_2 under the similar conditions. Additionally, the developed photocatalysts showed favourable recycle use potential because they could settle out of solution in less than 2 h after irradiation and their photocatalytic activities were still maintained >80% after four cycles of reaction. The developed photocatalysts were analyzed by various characterization techniques to obtain their physico-chemical properties. The coupling of studied metal oxides revealed in a reduction in the band gap of ZnO nanorod from 3.24 eV to 3.07–3.22 eV and hence, the

photocatalytic reaction was pushed into the visible region. The photocatalysts had high surface areas available for photocatalysis and were of N_2 adsorption-desorption isotherms of type IV with type H3 hysteresis loops. In contrast with the pure ZnO, the photoluminescence (PL) spectra of MO_x/ZnO photocatalysts indicated the dramatic decreased in their intensities. As for WO_3/ZnO photocatalysts, the PL intensity was the lowest. The enhancement in the WO_3/ZnO photocatalytic activity can be attributed to the high e^- and h^+ pair separation and the suitability of redox potential of the two semiconductors to produce highly active •OH radicals. This implication was proven by the radical scavenger and terephthalic acid–PL (TA–PL) experiments. Various operational parameters such as initial pollutant concentration, solution pH, calcination temperature and coupled metal oxide loading were investigated. The extent of degradation of EDCs and their mineralization were also verified further by HPLC and TOC analyses. The kinetics study revealed that the reaction order that best described the fluorescent light degradation of EDCs was first-order kinetic based on the Langmuir-Hinshelwood model. The electrical energy consumption per order of magnitude for degradation of EDCs was lower via the developed photocatalysts than that of the commercial TiO_2. Furthermore, the developed photocatalysts could be effectively utilize sunlight to degrade EDCs and their photocatalytic activities were again much superior to that of pure ZnO and commercial TiO_2 under the same conditions.

CHAPTER 1

INTRODUCTION

1.1 ENDOCRINE DISRUPTING CHEMICALS (EDCs) IN WASTEWATER

Water is the most precious natural resource in the world embracing over 75 % of the earth surface. The accessibility to safe drinking water is a high priority issue for the survival of human as well as wildlife. This is due to the fact that water resources such as rivers, lakes and oceans are being contaminated as a result of industrialization and urbanization processes leading to population growth, deforestation and pollution. Consequently, various international and local regulations are becoming stricter with time to control the amounts of pollutants discharged into the water as well as to ensure the quality of the treated effluents disposed into the aquatic environment. Nevertheless, many natural and synthetic pollutants are not generally controlled and monitored, although they are known or suspected to cause harmful ecological effects and can be deleterious to human health.

Widespread concerns are also being raised due to the increasing number of cases where such contaminants that are detected in surface water bodies have the potential to affect the reproduction, development and health of wildlife and even human. Evidence has emerged that these contaminants are able to interact with and disrupt the endocrine systems of living organisms. Thus, such pollutants are generally labeled as endocrine-disrupting compounds (EDCs) (Gultekin and Ince, 2007). The group of such substances increases with time and it includes industrial chemicals (phenols, polychlorinated biphenyls, chlorinated phenoxyacetic acid

herbicides, phthalates and parabens), synthetic pharmaceuticals, some heavy metals as well as the naturally occurring phytoestrogens (Walker, 2009).

Among the recognized EDCs, industrial chemicals such as phenols and chlorinated phenoxyacetic acid herbicides are believed to be responsible for majority of endocrine-disrupting effects on living organisms. They have high estrogenic activity even at the concentration ranging from several ng/L to mg/L (Bukowska and Kowalska, 2003; Tang *et al*., 2012). These compounds have been detected in different concentrations in surface waters all over the world. However, only several abatement technologies have been proposed.

Extensive literatures reveal that the detection of EDCs is a topic of great interest in environmental water contamination. Concern over the potential consequences of exposure to EDCs has garnered increasing attention of national and international organizations including the US Environmental Protection Agency (USEPA), European Commission, World Health Organization (WHO) and non-governmental organizations (Mendes, 2002; Matthiessen and Johnson, 2007). These organizations have implemented a number of regulations and projects with the objectives of establishing better understanding of the properties of the EDCs in order to improve the environmental protection and human health. To comply with stricter regulations, the development of new and sustainable techniques which are able to eliminate such pollutants is essential.

1.2 PHOTOCATALYSIS FOR WASTEWATER TREATMENT

A group of processes known as Advanced Oxidation Processes (AOPs) can be used to treat refractory pollutants. These processes include UV/H_2O_2, UV/ozone, direct ozonolysis and photocatalysis. However, they have the common characteristic,

i.e. the formation of short-lived oxygen containing intermediates such as hydroxyl radicals (•OH) or superoxide anion radicals (O_2•$^-$). These radicals are non-selective and highly reactive reagents. Among these options, photocatalysis is considered as one of the most promising technologies because it can be activated under low energy UV-A light with the help of semiconductor catalysts and it does not require the addition of any other strong oxidants. In addition, photocatalysis can also use sunlight as about 5% of the solar spectrum reaching the earth is in the UV-A wavelength range. Photocatalytic degradation process has several advantages, namely (Gaya *et al*., 2008; Malato *et al*., 2009):

(1) A wide variety of organic pollutants in aqueous and gaseous media can be completely degraded or mineralized.

(2) The photocatalysts are non-toxic, stable, biologically and chemically inert and available at low cost.

(3) Low energy UV light can be used to activate the photocatalyst and even utilization of natural sunlight.

(4) Photocatalytic reactions can occur in the presence of atmospheric oxygen and no other oxidant is required.

(5) This process is known as green technology because the degradation products (carbon dioxide and water) are environmentally harmless.

Titanium dioxide (TiO_2) is the most studied photocatalyst for the purpose of photodegradation of organic pollutants in wastewater (Fujishima *et al*., 2000; Chiou *et al*., 2008; Chen *et al*., 2010; Akpan and Hameed, 2011). Nevertheless, zinc oxide (ZnO) has recently been receiving attention from researchers. The energy levels for

the conduction and valence bands and the electron affinity of ZnO are similar to those of TiO_2. ZnO is a good semiconducting material for photocatalytic applications due to its unique chemical and physical properties, environmental stability and low cost in comparison to other metal oxides (Khodja *et al*., 2001; Lizama *et al*., 2002; Akyol *et al*., 2004). In some cases, ZnO catalysts can display higher degradation of organic pollutants than that of TiO_2 (Sakthivel *et al*., 2003; Daneshvar *et al*., 2004b; Palominos *et al*., 2009; Han *et al*., 2012). However, commercial exploitation of this new technology is still limited by the fact that ZnO is mostly active in the presence of UV light or the radiations with wavelengths below about 375 nm. Therefore, many researchers are focusing on the role of ZnO-based photocatalysts in order to shift the light absorption into longer wavelengths and to improve the photocatalytic processes.

1.3 PROBLEM STATEMENT

EDCs have garnered consideration nowadays due to they can exert hormonal imbalance activity and interfere with the endocrine system functions (Gultekin and Ince, 2007). Among various industrial chemicals, phenols and chlorinated phenoxyacetic acid herbicides are responsible for majority of endocrine disrupting effects on living organisms. Successful photodegradation of various organic pollutants including EDCs using UV light irradiation has been widely reported, whether for laboratory or pilot scale system (Trillas *et al*., 1996; Sleiman *et al*., 2007; Malato *et al*., 2009) as well as for industrial scale plant (Gogate and Pandit, 2004).

Nevertheless, in large scale application, artificial UV light sources may be prohibitively expensive in both capital and operating costs. Fluorescent light or sunlight irradiation has been considered as a practical and viable alternative despite of their low UV portion and band gap related limitation in ZnO photocatalysts.

Besides, fast recombination of photogenerated electrons and holes in ZnO photocatalysts is also of concern. As a result, many researchers have investigated various techniques to modify the ZnO photocatalyst in order to either extend the absorption region to longer wavelengths and/or to reduce the electron-hole recombination rate.

The manipulation of one dimensional (1D) ZnO nanostructures is proven to be an effective approach to reduce the recombination of photogenerated electron-hole pair (Wang *et al*., 2009c; Liu *et al*., 2011a). Hence, 1D ZnO has been synthesized with a variety of well-defined nanostructures with various morphologies such as nanotubes, nanorods, nanowires, nanobelts and nanonails for photocatalytic reactions (Lao *et al*., 2003; Sun *et al*., 2008; Li *et al*., 2010; Ma *et al*., 2011a ; Pyne *et al*., 2012). In particular, the ZnO nanorods has attracted much interest due to their advantages on: 1) enlarging the surface area for reactants access during the reactions (Zhao *et al*., 2011) and 2) maximizing the aspect ratio making them easily to be recovered after the reactions (Wang *et al*., 2008).

However, for the ZnO nanorods, the photocatalytic activity of ZnO with single modification (1M) is still not satisfactory and it can be attributed to short electron-hole pair lifetime. To further improve their photocatalytic activity, the preparation of ZnO involving double modifications (2M) has attracted much attention (Nayak *et al*., 2008; Pant *et al*., 2011; Saravanan *et al*., 2011). Semiconductor materials coupled with ZnO photocatalysts have particularly proved to be promising options in inhibiting the electron-hole pair recombination as the coupled semiconductors can act as irreversible electron and/or hole sinks. Moreover, some researchers reported that the coupled semiconductor materials with two

different energy-level systems can reduce the band gap and extend the light absorbance range to visible light region (Li *et al*., 2011a; Saravanan *et al*., 2011).

In developing efficient ZnO coupled catalytic system, the photocatalytic mechanism is regarded to be an important issue (Robert, 2007; Chen *et al*., 2008; Malato *et al*., 2009). Thus far most of the ZnO coupled systems were limited to the transport of electrons or holes between the coupled metal oxide and ZnO and their relative energy band positions for succession in the creation of reactive radical species is scarcely studied. On the other hand, in term of coupled metal oxide selection (MO_x = CuO, WO_3 and Nb_2O_5), no report has been seen on WO_3 and Nb_2O_5 coupled with ZnO nanorods and their photocatalytic properties. This present work was therefore aimed to develop highly efficient visible-light MO_x/ZnO photocatalysts based on the understanding of the photocatalytic reaction mechanism as well as their photocatalytic performance on the fluorescent light and sunlight degradation of phenol and 2,4-dichloropehoxyacetic acid (2,4-D). The obtained results will also provide insight in correlation of the relative energy band positions between the coupled metal oxide and ZnO nanorods for the reactive radical species production during the photocatalytic reaction.

1.4 RESEARCH OBJECTIVES

The present research study is aimed at developing metal oxide coupled ZnO nanorod (MO_x/ZnO) photocatalysts for photocatalytic degradation of phenol and 2,4-D under fluorescent light and sunlight irradiation. The specific objectives are:

i. To develop a series of MO_x/ZnO photocatalysts using different coupled metal oxides (MO_x = CuO, WO_3 and Nb_2O_5) via a hydrothermal–deposition method.

ii. To characterize the physical and chemical properties of developed photocatalysts.

iii. To examine the activity and effectiveness of the coupled photocatalysts on degradation of phenol and 2,4-D under fluorescent light and sunlight irradiation.

iv. To evaluate the process parameter effects and to monitor the evolution of degradation intermediates and inorganic ions during the photocatalytic process.

v. To assess the kinetic studies and electrical energy evaluation in the photocatalytic degradation of phenol and 2,4-D.

1.5 SCOPE OF THE STUDY

The present study covers the photocatalyst development, photocatalyst characterization, process analysis, intermediate detection, kinetic study as well as electrical energy evaluation for photocatalytic degradation of EDCs, phenol and 2,4-D under fluorescent light and sunlight irradiation. The EDCs concentrations in the solution are monitored using a high performance liquid chromatography (HPLC) and total organic carbon (TOC) analyzers. The developed photocatalysts are characterized using X-ray diffraction (XRD), transmission electron microscopy (TEM), high resolution transmission electron microscopy (HRTEM), energy dispersive X-ray (EDX), UV–visible diffuse reflectance spectroscopy (UV–vis DRS), nitrogen physisorption and photoluminescence (PL) spectroscopy.

The photocatalysts development is started with the preparation of ZnO nanorods using commercial ZnO powder in aqueous H_2O_2 solution via a hydrothermal method. The possible growth mechanism for the nanorod structures has been proposed. This is followed by the addition of coupled metal oxides such as CuO, WO_3 and Nb_2O_5 using a hydrothermal-deposition method. These coupled metal oxides have been selected because they have different energy levels, which are effective to act as charge separators in the coupled ZnO system. The effects of coupled metal oxide loading and calcination temperature on the activity of the coupled photocatalysts have been investigated. In this regard, the physical and chemical properties of the obtained coupled photocatalysts have been characterized using XRD, TEM, HRTEM, EDX, UV–vis DRS, nitrogen physisorption and PL analyses. Those specific properties have been further correlated with their fluorescent light and sunlight photoactivities. The photoactivities have been demonstrated based on the degradation of aqueous phenol and 2,4-D as the model EDC pollutants.

In this study, effects of initial substrate concentration and solution pH on the EDCs degradation have been examined. These factors are chosen because they are generally reported to have significant influence on the photocatalytic process. This is followed by the investigation on the intermediates that are formed in the EDCs degradation process. To gain further insights into the photocatalytic mechanism under irradiation, the roles of numerous oxidative species such as h^+, •OH and O_2•$^-$ radicals has been studied with the use of radical scavengers and terephthalic acid-photoluminescence (TA−PL) test. A kinetic study has also been carried out to obtain the reaction order, reaction rate and rate constant of the EDCs degradation processes. Finally, an electrical energy evaluation has been performed for the EDCs degradation processes using the developed photocatalysts.

1.6 ORGANIZATION OF THE THESIS

This thesis consists of five chapters. Chapter 1 (Introduction) presents the environmental problems associated with the released of industrial wastewater into the environment. It also points out the merits of the photocatalysis over other methods. This chapter includes the problem statement, the objective of the research, scope and justification for embarking upon the research.

Chapter 2 (Literature review) extracts some relevant information from past reported research studies for the photocatalyst development. It presents the properties of ZnO and possible routes for the enhancement of the ZnO photocatalysts activity. The toxicology of EDCs and EDCs remediation technologies are also discussed.

Chapter 3 (Materials and Methods) describes in details the materials and chemicals used as well as the research methodologies employed in the present study. Details of the experimental setup including a step-wise description of the photocatalyst development, process conditions and photocatalyst characterizations are outlined in this chapter.

Chapter 4 (Results and Discussion) is the main body of the thesis which discusses, interprets and analyses the results obtained in the present investigations. This chapter comprises of several sections, which are the coupled photocatalysts development, characterization of coupled photocatalysts, photodegradation of phenol and 2,4-D under fluorescent light and sunlight irradiation, proposed photocatalytic mechanism, process analysis, intermediate identification, kinetic analysis and electrical energy evaluation.

Chapter 5 (Conclusions and recommendations) summarizes the conclusions drawn from this study. Recommendations for future work based on findings made in this research are also presented in this chapter.

CHAPTER 2

LITERATURE REVIEW

2.1 PHOTOCATALYSIS

Photocatalysis can be defined as the acceleration of a photochemical reaction by the presence of a catalyst that in turn lowers the activation energy for the primary reaction to occur. Photocatalytic degradation which is also known as heterogeneous photocatalysis has been used since mid-1970s to decontaminate water from harmful microorganisms. In classical heterogeneous photocatalytic process, photoinduced chemical reactions or molecular transformations occur on the surface of a catalyst. This overall process can be separated into five independent steps: (1) transfer of pollutants to the surface of the catalyst, (2) adsorption of the pollutant on the surface, (3) reaction on the adsorbed phase, (4) desorption of the product and (5) removal of the product from the interfacial region (Herrmann, 1999). The mass transfer steps (1) and (5) are dependent on the reactant/product concentration as well as photocatalyst loading and particle size. Meanwhile, steps (2), (3), and (4) depend on the chemical compatibility of reactant and product molecules with the active sites. One of these steps will control the overall reaction rate. It is essential to understand these controlling steps so that the photocatalyst or operating conditions can be varied to obtain optimum performance.

2.1.1 Principles of photocatalytic reaction

The photocatalytic reaction occurs in step (3) in which a semiconductor upon absorption of a photon with suitable energy can act as a photocatalytic substrate by producing highly reactive radicals that can oxidize organic pollutants. The

mechanism of photocatalytic degradation on the surface of ZnO catalyst is given below in Equations (2.1)–(2.11).

$$ZnO + h\nu \rightarrow ZnO\ (e^- + h^+) \quad (2.1)$$

$$ZnO\ (e^- + h^+) \rightarrow ZnO + \text{heat (or light)} \quad (2.2)$$

$$h^+ + OH^-_{ads} \rightarrow \bullet OH \quad (2.3)$$

$$h^+ + H_2O_{ads} \rightarrow \bullet OH + H^+ \quad (2.4)$$

$$O_{2ads} + e^- \rightarrow O_2\bullet^- \quad (2.5)$$

$$O_2\bullet^- + H^+ \rightarrow HO_2\bullet \quad (2.6)$$

$$O_2\bullet^- + HO_2\bullet \rightarrow HO_2^- + O_2 \quad (2.7)$$

$$2HO_2\bullet \rightarrow H_2O_2 + O_2 \quad (2.8)$$

$$H_2O_2 + O_2\bullet^- \rightarrow OH^- + \bullet OH + O_2 \quad (2.9)$$

$$H_2O_2 + e^- \rightarrow OH^- + \bullet OH \quad (2.10)$$

$$H_2O_2 + h\nu \rightarrow 2\bullet OH \quad (2.11)$$

The photoreactions in Equations (2.3)–(2.11) indicate the critical role of the interaction between the photocatalyst with other adsorbed molecules. Photoactivated semiconductor surfaces can attract electron donors and acceptors through both chemical and electrostatic forces including van der Waals forces, induced dipole-dipole interactions, dipole-dipole interactions and hydrogen bonding (Carp *et al.*, 2004).

2.1.1.1 Band gap excitation

Equation (2.1) indicates that the theory behind photocatalysis can be explained based on basic semiconductor principles. When a photocatalyst is irradiated with photons with energies equal to or greater than that of its band gap, E_g (eV) an e^- is promoted to the conduction band (CB), leaving behind an h^+ in the

valence band (VB). The pair of photoexcited charge carriers that happen within a particle is also known as an electron-hole pair (EHP). The minimum wavelength of the photon irradiation that is required to promote an EHP depends on E_g of the photocatalyst and it is given in Equation (2.12) (He *et al*., 2011):

$$E_g = 1240/\lambda \quad (2.12)$$

where, λ is the minimum wavelength (nm) of photon irradiation to induce photoexcitation of a semiconductor with band gap E_g (eV). The formation rate of EHPs is first governed by irradiation conditions such as light intensity and its wavelength and followed by intrinsic properties of a semiconductor such as their E_g, crystal configuration, surface area, porosity and so on (Bhantkhande *et al*., 2001; Carp *et al*., 2004).

Figure 2.1 illustrates several possible reaction pathways that may occur on EHPs once they are generated by irradiation at suitable energy. Reaction (1) is the formation of an EHP upon absorption of photon with energy equal to or greater than the E_g of the semiconductor. Reactions (2)–(5) depend on bulk and surface properties of the photocatalyst. Reaction (2) occurs when an electron acceptor (*A*) is reduced by removing a migrating e^- from the surface of the particle. Reaction (3) is an oxidation reaction that occurs when an e^- from a donor species (*D*) combines with an h^+ and migrates to the surface. In the absence of such acceptors and donors, the EHP will undergo fast recombination. Reactions (4) and (5) can be respectively described as volume and surface recombination and are the dominant fate of EHPs, resulting in low photocatalytic efficiencies.

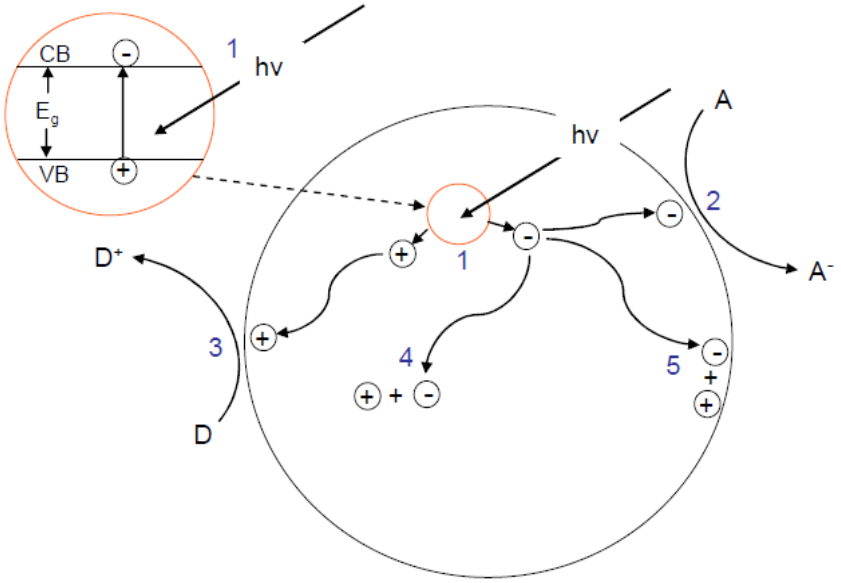

Figure 2.1: Schematic photoexcitation of the EHPs and the subsequent redox reactions (Linsebigler *et al*., 1995).

2.1.1.2 Band edge position

The semiconductor band gap is defined as the energy difference between the bottom of the VB edge and the top of the CB edge. Knowledge of the band edge positions at the surface is very useful since they reveal thermodynamic limitations for photoreactions that can be carried out by the photogenerated charge carriers in a semiconductor. For example, if the reduction reaction is required. The CB edge of the semiconductor must be positioned higher than the reduction potential of the target molecule. On the contrary, if the oxidation reaction is desired by the photocatalyst, the VB edge of the semiconductor must be positioned favorably relative to the oxidation potential of the absorbed molecule. The band edge energies for several important semiconductors are shown in Figure 2.2.

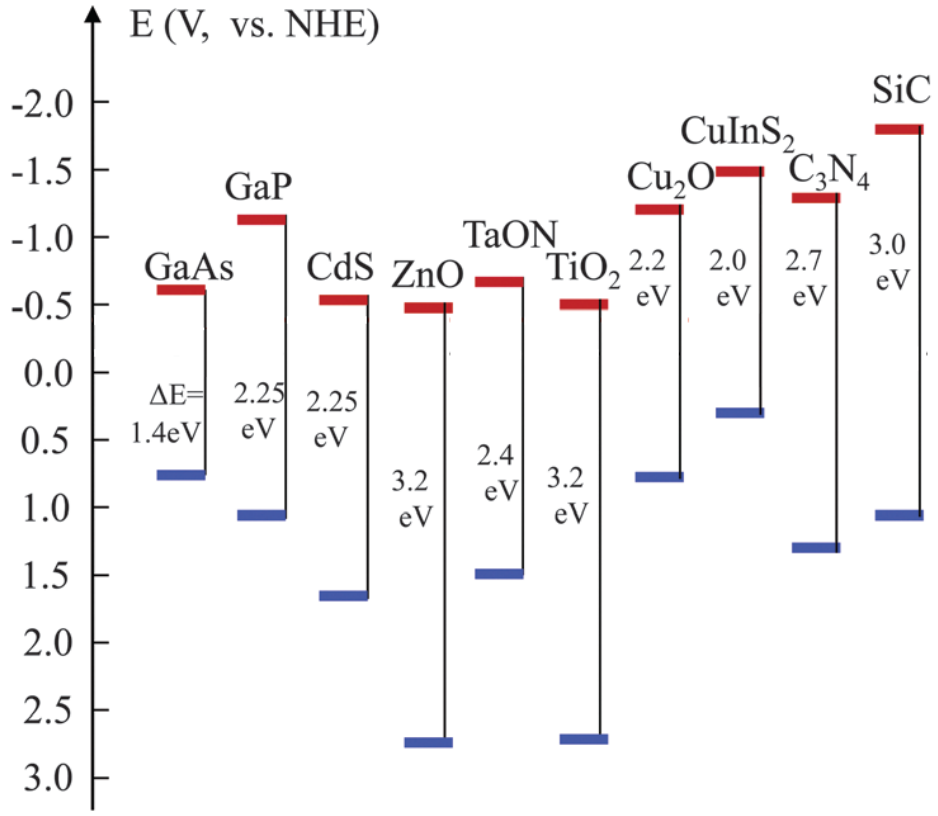

Figure 2.2: Band gap energy and band edge positions for selected semiconductors (Liu *et al*, 2014).

2.1.1.3 Electron–hole pair (EHP) recombination

In the competition with charge transfer to adsorb species, there is possibility that the EHP recombination occurs and decreases the photocatalytic efficiency. The recombination can occur on the surface or volume of the semiconductor with the release of heat or light as shown in Equation (2.2). The EHP recombination process itself resulted when the EHP time is shorter than the time takes by the charge carrier to diffuse to the surface. The time scales for the interfacial transfer of h^+ to the donor species and the interfacial charge transfer of e^- to the electron acceptor are ~100 nanosecond and microsecond, respectively. Nevertheless, it is generally accepted that the EHP recombination occur in the timeframe of picosecond and nanosecond, depending on the type of semiconductor material and its particle size (Linsebigler *et al*., 1995).

2.1.1.4 Role of photogenerated electron and hole in photocatalysis

For a semiconductor to have high quantum efficiency, its photogenerated charge carriers must transfer to have interaction with an adsorbed species on the surface of the particle. These e^- transfer to the surface can suppress the EHP recombination (Gaya and Abdullah, 2008; Malato *et al*., 2009). The photogenerated e^- that are able to transfer to the surface are primarily used in the reduction of O_2 to produce $O_2\bullet^-$ radicals (Equation (2.5)), which can in turn stimulate other radical chain reactions involving hydroperoxyl radical ($HO_2\bullet$), •OH radical and hydrogen peroxide (H_2O_2) (Gogate and Pandit, 2004; Chong *et al*., 2010).

On the other hand, the photogenerated h^+ that are able to migrate to the surface can react with the adsorbed H_2O or OH^- groups to generate the •OH radicals (Equations (2.3) and (2.4)). These •OH radicals have been considered to be responsible for the degradation of organic compounds due to their high oxidation capability (Fujishima *et al*., 2000; Mrowetz *et al*., 2004). The •OH radical formation on photocatalyst surface in solution has been performed through simple terephthalic acid–fluorescence (TA–FL) technique. Using this technique, the intensity of the peak attributed to 2-hydroxylterephthalic acid was known to be proportional to the amount of •OH radicals formed (Ishibashi *et al*., 2000; Qiu *et al*., 2008; Zhang *et al*., 2009). Electron spin resonance (ESR) has also been used to study the radical oxidative species detection in solutions. This technique allowed the presence of •OH and $O_2\bullet^-$ radicals in photocatalytic systems to be monitored (Liu *et al*., 2000; Fu *et al*., 2006; Shang *et al*., 2012).

Additionally, the mediation of oxidative species in the photocatalytic reaction has also been evidenced by scavenger-loaded conditions (Palominos *et al*., 2008; Wang and Lim, 2011; Liu *et al*., 2012b). As a consequence of scavenging, the

photocatalytic reaction suppressed. The extent of decrease in the degradation induced by scavenger revealed the importance of the corresponding oxidative species. Hence, it is essential to understand the roles of oxidative species produced by the photogenerated e^- and h^+ in the photocatalytic reactions.

2.1.2 Basic properties of ZnO

ZnO with an appearance of white powder is insoluble in water and alcohol. It naturally occurs as the mineral zincite, which exists in three structures: hexagonal wurtzite, zincblende and rocksalt (Ozgur *et al*., 2005). Crude ZnO is commercially produced via French process in which the metallic zinc is vapourized in a large container by external heating. In an adjoining off-take pipe or combustion chamber, the vapour is burned off in the air to a fine ZnO powder (Harper, 2001). Meanwhile, the American process, oxidized ores of roasted sulfide concentrates are mixed with anthracite coal (carbon additive) and smelted in a furnace. The coal together with the products of partial combustion mainly carbon monoxide will reduce the ore to metallic zinc, which is released as vapour. The zinc vapour is then re-oxidized by lower temperature air to form ZnO particulate. The purity of the ZnO produced by this process is rather inferior to that from the French process as it generally contains low levels of lead and sulphur contents (Porter, 1991; Harper, 2001).

At ambient pressure and temperature, ZnO crystallizes in the hexagonal wurtzite structure (as recorded in Figure 2.3) with lattice parameters $a = b = 0.3296$ nm and $c = 0.5207$ nm (Ozgur *et al*., 2005). This structure can be illustrated as a number of two type planes consisting of tetrahedrally coordinated O^{2-} and Zn^{2+} ions stacked alternately along the *c*-axis. In addition to wurtzite phase, ZnO is also known to crystallize in the cubic zincblende and rocksalt (NaCl) structures, which are

illustrated in Figure 2.3. Zincblende ZnO is stable only by growth on cubic structures, while the rocksalt structure is a high-pressure metastable phase forming at ~10 GPa and cannot be epitaxially stabilized (Ozgur *et al*., 2005).

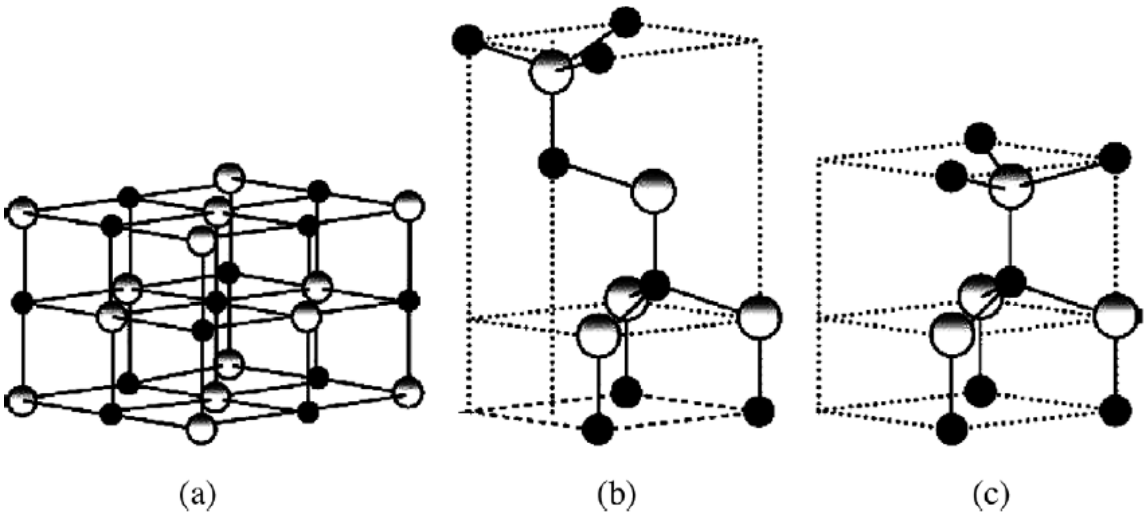

Figure 2.3: ZnO crystal structures: (a) cubic rocksalt; (b) cubic zincblende; (c) hexagonal wurtzite. The shaded white and black spheres denote Zn and O atoms, respectively (Ozgur *et al*., 2005).

ZnO has a wide band gap of about 3.20−3.37 eV at room temperature (Zhang *et al*., 2003; Kumar *et al*., 2012). It has exciton binding energy as high as 60 meV, which is much higher than that of room temperature thermal excited energy (25 meV). Thus, theoretically, it can harvest high efficient UV exciton emission and laser at room temperature, which strongly prompts the applications of opto-electronic in the fields of optical waveguide, optical switches and transparent ultraviolet protective conducting films (Porter, 1991). Moreover, the melting point of ZnO is 1975^{o}C, which determine its high thermal and chemical stability. In addition, ZnO owns a huge potential commercial value due to its cheaper price, abundant resources in the nature, environmental friendly and simple fabrication process (Bitenc *et al*., 2013).

Therefore, ZnO has been a new focus in the fields of sensor materials, solar cells and photocatalysts.

2.1.3 Radiation sources

Radiation sources play a pivotal role in the performance of photocatalytic reaction. Normally, the selection of particular lamp is made on the basis of the reaction energy requirement of particular catalyst. There are six types of radiation sources: 1) arc lamps, 2) fluorescent lamps, 3) incandescent lamps, 4) lasers, 5) light-emitting diodes (LEDs) and 6) solar irradiation (Augugliaro *et al*., 2010).

In general, arc lamps are the most common used source of UV and visible irradiations for photocatalytic process. In arc lamps, the emission is obtained by the activation of a gas by collisions with e^- accelerated by an electric discharge between two electrodes, typically made of tungsten (Augugliaro *et al*., 2010). The activated gases are usually mercury and/or xenon vapour. For mercury lamps based on the pressure of Hg, these lamps can be divided into low pressure Hg lamps (pressure up to 0.1 pa, emission mainly at 253.7 nm and 184.9 nm), medium-pressure Hg lamps (pressure ranging from 100 to several hundred pa, emission from 300 nm to 1000 nm) and high-pressure Hg lamps (pressure up to Mpa or higher, emission from 200 nm to 1000 nm). Generally, arc lamps are high power and need to be cooled by air or circulating liquid around them. Moreover, a large proportion of light energy is also not useful for the photocatalytic process as they can be converted to thermal energy (Ren *et al*., 2010).

On the other hand, fluorescent lamps (FLs), which are used as household illumination, offer a new promising source because of their safety, long time and efficiency electricity to light conversion (Ren *et al*., 2010). FLs are filled with gas

mixture of low pressure mercury vapour and argon (or xenon). The inner surface of the lamp is coated with fluorescent coating made of varying blending of metallic and rare-earth phosphor salts. When the light is turned on, the tungsten cathode is heated to produce e^- and this e^- will collide with the gases to emit light. Fluorescent lighting is efficient because low pressure Hg emits about 65% of their total light at 254 nm (Augugliaro *et al*., 2010). The UV light is then absorbed by the fluorescent coating, which re-radiates the energy at higher wavelengths to emit visible light (Kirchnerova *et al*., 2005; Nawi *et al*., 2011). Therefore, if the intensity of light available from ordinary FLs would be sufficient to degrade organic pollutants, they can also provide the opportunities for the application of photocatalytic process in the indoor environments.

2.1.4 ZnO photocatalytic oxidation of organic pollutants

A wide range of toxic organic pollutants have been treated by photocatalytic processes to test the general applicability of the method. Halogenated hydrocarbons are readily oxidized in aqueous suspension of ZnO photocatalyst with general stoichiometry as shown in Equation (2.13):

$$C_xH_yCl_z + [x + ((y - 4)/4)]\ O_2 \rightarrow xCO_2 + zHCl + ((y - 2)/2)\ H_2O \quad (2.13)$$

Phenolic compounds such as phenol can be also photocatalytically oxidized following the stoichiometry as shown in Equation (2.14) (Chiou *et al*., 2007):

$$C_6H_5OH + 7O_2 \rightarrow 6CO_2 + 3H_2O \quad (2.14)$$

Dyes, pesticides and aliphatic carboxylic acids are another classes of organic pollutants that can be degraded using ZnO photocatalysts. Table 2.1 lists the different types of organic pollutants that have been degraded with ZnO photocatalysis.

Table 2.1: Examples of ZnO photodegradation of various organic pollutants.

Class of organic	**Example**	**Reference**
Alkanes	Hexane	Saucedo-Lucero and Arriaga (2013)
Aliphatic aldehydes	Acetaldehyde	Wahab *et al*. (2013)
Aromatics	Naphthalene, Anthracene,	Pal and Sharon (2002)
Phenolic compounds	Catechol, Phenol, 4-Acetylphenol, 2-Phenylphenol	Khojda *et al*. (2001), Kansal *et al*. (2007a), Sobana *et al*. (2008), Shukla *et al*. (2010)
Halophenols	2,4,6-Trichlorophenol, 4-Chlorophenol, 2,4-Dichlorophenol	Gaya *et al*. (2009), Gaya (2010), Gaya *et al*. (2010)
Aromatic carboxylic acids	Pentafluorobenzoic acids, 3,4-Dihydroxylbenzoic acid, Salicylic acid	Ravichandran *et al*. (2007), Nayak *et al*. (2008), Rao *et al*. (2009)
Herbicides	Metamitron, Triclopyr	Poulios *et al*. (1998), Mijin *et al*. (2009)
Pesticides	Triadimenol, Methyl Parathion, Dimethoate	Evgenidou *et al*. (2005), Evgenidou *et al*. (2007), Navarro *et al*. (2009)
Insecticides	Phosphamidon, Monocrotophos Diazinon	Rabindranathan *et al.* (2003), Anandan *et al*. (2007a), Daneshvar *et al*. (2007)
Dyes	Ethyl Violet, Methyl orange, Rhodamine 6G, Indole	Chen (2007), Kansal *et al*. (2007b), Samah *et al*. (2011)

The non-selective and total photodegradation properties of the ZnO particles in aqueous suspensions are related to the strong oxidative species formed as previously described during the photocatalytic process. Nevertheless, there are also several shortcomings appearing during the practical application of ZnO:

- The E_g of ZnO is wide that light absorption is limited to the UV region.
- Photogenerated EHPs easily recombined, which restrained the photocatalytic efficiency.

Thus, morphological modification and semiconductor coupling have been suggested to improve the photocatalytic efficiency of ZnO.

2.2. IMPROVING ZnO PHOTOACTIVITY VIA MORPHOLOGICAL MODIFICATION

Semiconductor nanostructured materials are a new class of materials having dimensions in the 1–100 nm range, which provide one of the greatest potentials for improving performance and extending capabilities of products in a number of industrial sectors (Yi *et al*., 2005; Fang *et al*., 2011). These nanostructures can be divided into zero-dimensional (0D when they are uniform), one-dimensional (1D when they are elongated), two-dimensional (2D when they are planar) and three-dimensional (3D when they are ordered structures and several hierarchical architectures). The 1D ZnO nanostructures have attracted much attention due to their many unique properties and the possibility that they may be used in electronics, optoelectronics, piezoelectrics, nanogenerators, biomedicals, electromechanical nanodevices as well as their use as environmental catalysts (Comini *et al*., 2009; Zhai *et al*., 2009). Various kinds of ZnO 1D nanostructures have been realized such as nanowires, nanorods, nanobelts, nanotubes, nanocombs, nanoneedles, nanobridges, nanonails, nanowalls and nanohelixes (as illustrated in the Figure 2.4).

In the photocatalytic reaction, the ZnO 1D nanostructures have revealed a good performance. On the one hand, they have larger surface area than the microscale powders, which enlarges their contact surface during the reaction. On the other hand, compared to nanoparticles, their higher length-width ratio enables them to be easily filtered out after the reaction. Several researchers have also added that

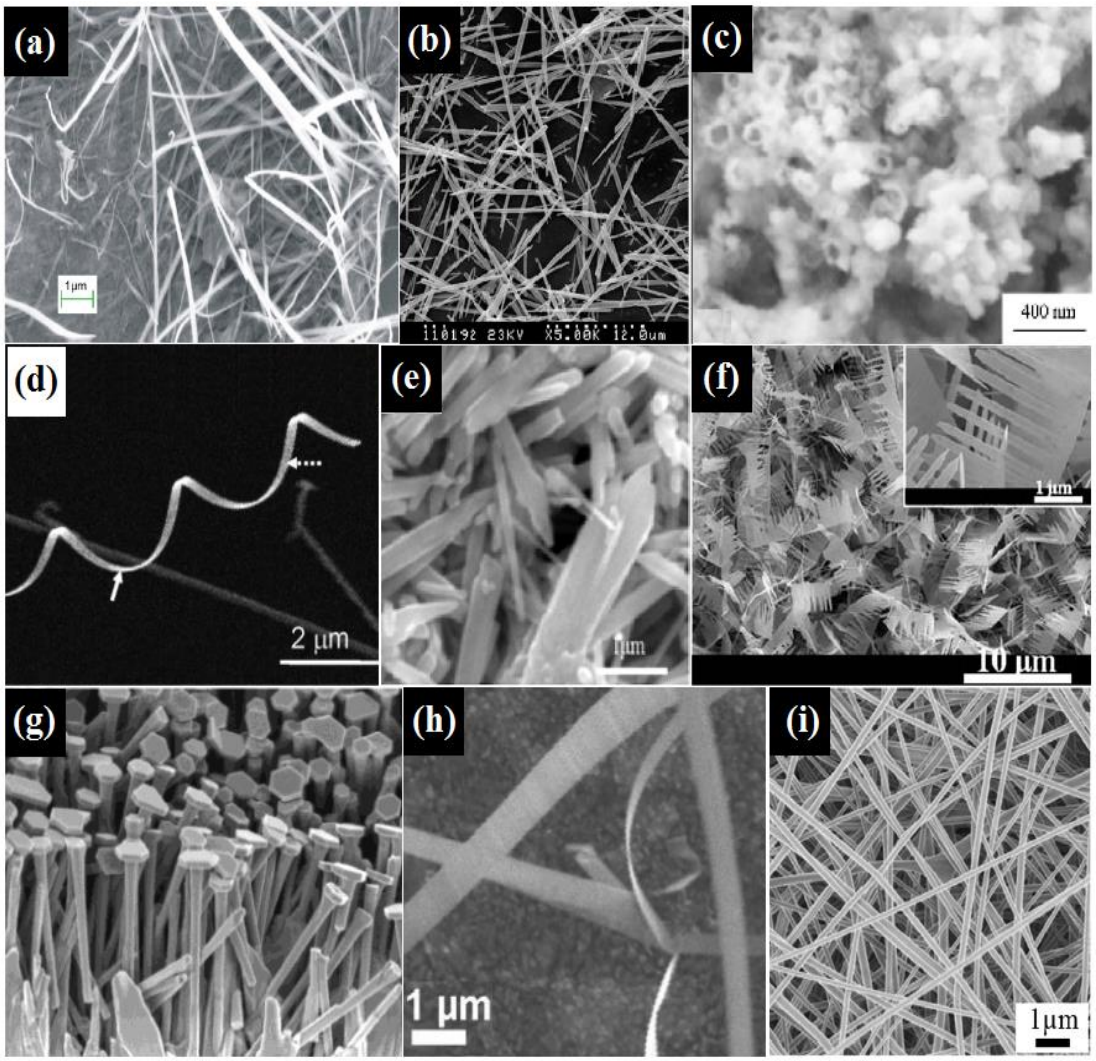

Figure 2.4: ZnO 1D structures (a) nanowire (Pyne *et al*., 2012), (b) nanoneedle (Xie *et al*., 2011), (c) nanotube (Li *et al*., 2010), (d) nanohelice (Gao *et al*., 2006) (e) nanorod (Ma *et al*., 2011a), (f) nanocomb (Umar, 2009), (g) nanonail (Lao *et al*., 2003), (h) nanobelt (Sun *et al*., 2008) and (i) nanofiber (Li *et al*., 2011a).

these nanostructures have others special merits over nanoparticles such as low number of grain boundaries, enhancing the light utilization rate and avoiding the recombination of EHP (Mohajerani *et al*., 2009; Zhou *et al*., 2010; Liu *et al*., 2011). This strongly adds mark to ensure the ZnO 1D nanostructures to be a good catalyst for photocatalytic process. Table 2.2 lists the photocatalytic degradation of organic pollutants via ZnO 1D nanostructures.

Table 2.2: Photocatalytic degradation of organic pollutants via 1D ZnO nanostructures.

Catalyst	**Method preparation**	**Type of pollutant**	**Operating condition**	**Results and comment**	**Reference**
Nanoparticle, flower-like, nanorod, micro-sphere	Hydrothermal	C.I. Acid Red 27	Sunlight (200–250 W/m^2); 50 ppm of Acid Red; volume = 100 mL; treatment time = 120 min; catalyst = 0.1 g.	Degradation rate of 0.0168, 0.0077, 0.0195 and 0.0045 min^{-1} for nanoparticle, flower-like, nanorod and micro-sphere, respectively.	Mohajerani *et al*. (2009)
Nanoneedle, nanoparticle, TiO_2 film, flower-like	Thermal evaporation of zinc powders	Methylene Blue (MB)	20 W Hg lamp (λ = 254 nm); 10 mg/L of MB; volume = 60 mL; treatment time = 240 min.	96%, 75%, 62% and 56% degradation of MB for nanoneedle, nanoparticle, TiO_2 film and flower-like, respectively.	Yan *et al*. (2009)
Nanotube	Microwave hydrothermal	Methyl Orange (MO)	400 W UV light (λ = 365 nm); 10 mg/L of MO; volume = 200 mL; treatment time = 1 60 min; catalyst = 25 mg.	100% degradation of MO for both nanotube and commercial ZnO. Faster degradation rate was observed for nanotube.	Chen and Lo (2011)
Nanowire	Carbothermal reduction	Methylene Blue (MB)	1000 W Xe lamp (λ = 320–400 nm, 8 mW/cm^2); 10 mg/L of MB; volume = 100 mL; treatment time = 60 min; catalyst = 20 mg.	Degradation rate of 1.86 h^{-1} of MB within 60 min.	Ma *et al*. (2011b)

Table 2.2: Continued

Nanoparticle, nanorod, nanocauliflower, nanosheet-like	Template assisted growth	Methylene Blue (MB)	Sunlight (10 A.M.–3 P.M.); 5 ppm of MB; volume = 50 mL; treatment time = 75 min.	Degradation order: nanorod > nanoparticle > nanosheet-like > nanocauliflower.	Sabbaghan *et al*. (2012)
Nanorod, nanoflower, particle	Hydrothermal	Methyl Orange (MO)	250 W Hg lamp (λ = 365 nm); 10 mg/L of MO; volume = 200 mL; treatment time = 70 min.	Degradation order: nanorod > nanoflower > particle.	Ma *et al*. (2011a)
Nanobelt arrays rod/comb-like, particle film	Carbothermal reduction	Methyl Orange (MO)	200 W Hg lamp (λ = 365 nm); 15 mg/L of MO; volume = 100 mL; pH = 7; treatment time = 300 min.	59%, 71% and 94% degradation of MO using particle film, rod/comb-like and nanobelt array, respectively.	Sun *et al*. (2008)